



Improved Process for Laser-Assisted, In Situ, Multi-Stage Wear Measurement of Simultaneously Wearing Counterparts

Paul Christian Sager¹ · Birgit Schaedel¹ · Roland Kral¹ · Rainer Adelung²

Received: 31 July 2025 / Accepted: 22 October 2025 / Published online: 31 October 2025
© The Author(s) 2025, modified publication 2026

Abstract

Accurate in situ wear measurements of polymer-polymer wear combinations using techniques like ball-on-prism tribometers pose a significant challenge. Simultaneous wear of both counterparts complicates obtaining continuous wear data without interrupting experiments to perform slow, intermediate measurements. Building on Harden et al. (Tribol Lett 71(3):1–14, 2023), this work develops an accurate, low-noise measurement approach to enable reliable in situ measurements. The method employs a laser line scanner and a precision linear axis for accurate positioning within the test stand, complemented by an algorithm for debris detection and data smoothing to minimize noise from wear residue. This approach achieves up to a 98% reduction in peak-to-peak noise levels, enabling high-resolution measurements and supporting parallel experiments with various polymer-polymer wear combinations. Unlike existing non-in situ methods, this technique offers efficient and accurate in situ wear measurements, advancing tribological research and polymer material testing.

Keywords Tribology · Wear · Wear-differentiation · Polymer-polymer · Polymer-tribology · Wear-measurement

1 Introduction

Polymers have been used as materials for tribological applications for many years. The usage of polymers is mainly focused on low to medium temperature, speed and load applications with the benefits of reducing the need of maintenance measures, such as lubrication [1–3].

Using the process of additive manufacturing, also known as 3d printing, new possibilities for manufacturing complex mechanisms arise. When manufacturing mechanisms using additive manufacturing, one has the possibility to incorporate printed joints to allow the mechanism to be used directly after printing without any additional assembly. Another use-case for 3d printing is the manufacturing of complex bearing geometries. There are multiple different 3d-printable materials available, that have been tailored and optimized to suit the mentioned tribological applications, such as iglidur[®]

i150 filament for Fused Deposit Modeling (FDM) processes [4].

In this work, wear is considered as material permanently leaving the contact surfaces. This is referred to as the third body model in literature [5]. Wear volume is then defined as the volume of said material loss. There are many different wear measurement devices and setups found in literature to test various wear conditions, such as lubrication, introduction of abrasive media or simply measuring the wear that two materials impose on each other. Most of the measurement techniques consist of a sample that is pressed onto another sample with a defined normal force and moved, oscillated or rotated to create friction and wear. A few examples of this are the Twin Disk Tribometer, where two disks are pressed together radially and rotated against each other, the Four- or Three Ball Tribometer, where three or four balls are pressed against each other and rotated [6, 7]. Most of these measurement techniques can be set up to record data during the measurement. This data would be the indentation depth of the wearing bodies for most test setups.

As Harden et al. point out in their publications, with the indentation depth of the ball into the prism or vice versa as the only source of data, one cannot differentiate between ball and prism wearing. In order to determine the true wear volume of both the ball and the prism, additional information

✉ Paul Christian Sager
paul.sager@th-luebeck.de

¹ Department of Mechanical Engineering and Business Administration, Technische Hochschule Luebeck, Moenkhofer Weg 239, 23562 Luebeck, Germany

² Faculty of Engineering, Christian-Albrechts-University, Kaiserstrasse 2, 24143 Kiel, Germany

is needed about the wearing geometry. After the experiment, the wear volume of the prism can be calculated by mapping the topography of the prism surface. One could also weigh the samples to obtain the amount of worn-away material. With this additional information, also the wear volume of the ball can be calculated. The downside of this procedure is, that one does not obtain data of the different wear states during the measurement, making this process not in situ but postmortem. This means that the true wear curves can only be approximated using a linear function or by interpolating a curve in between the ball- and the prism-wear curve. For more accurate approximations of the true wear curve of the system, one would have to remove the prisms at fixed times during the experiment, perform a surface scan, and remount the prism in the same place and orientation than before to archive reliable results. This presents multiple challenges. The first being the prolonged experiment duration caused by the constant mounting and unmounting of the samples, the other one being the increased uncertainty caused by the inaccuracy in remounting the samples and repeating run-in phases [8, 9].

There are multiple approaches for measuring the true wear volume over time, which all suffer from the issue of either only being able to measure one wearing geometry at the time or needing to unmount the sample for geometry measurements [10–13].

Harden et al. proposed a method to differentiate between the wear volumes of the individually wearing partners without the need to stop the measurement and to unmount the samples. In their work, the authors used a VPS6 ball-on-prism tribometer, manufactured by Dr. Tillwisch GmbH, to conduct the wear measurements. The tribometer is equipped with linear displacement transducers to record the relative indentation depth of the ball into the prism and vice versa. The data coming from the transducers are digitized and recorded using a Spider8 amplifier by Hottinger Brüel & Kjær GmbH. By utilizing a scanCONTROL 2900 10/BL laser profile scanner (LPS) from Micro-Epsilon Messtechnik GmbH & Co. KG, the ball's geometry is measured during fixed time intervals and saved to a text file. With the geometry information of the ball over the time and the indentation depth over the time the true wear volume of both the ball and the prism is calculated. As a result the true wear volume of the ball and the prism can be plotted over the time of the experiment [8].

As the authors point out in the conclusion, the accuracy of this setup is too low for measuring wear combinations with a small wear volume [8]. According to Harden et al., the main reasons for this inaccuracy are the varying rotational speed of the ball, combined with the balls radial runout when rotating [8].

The results presented in the work of Harden et al. show different levels of noise depending on the wearing- and

loading conditions. The author conducted different test runs for all possible wearing states. An AlMg3 ball against no prism was used to create no wear, an AlMg3 ball against a Polyethylene-terephthalate-glycol modified (PETG)- Polytetrafluoroethylene (PTFE) prism to create only prism wear, a Polyamide 66 (PA66) ball against a 100Cr6 prism to create only ball wear and a PETG-PTFE ball against a PLA prism to wear both counterparts. Table 1 shows the approximate noise levels at the beginning of the experiment, as seen from the graphs presented in the work of Harden et al.

This work proposes an improved approach and measurement setup by addressing the challenges pointed out in the work of Harden et al. aiming to reduce the noise to signal ratio such, that also wear combinations with a lower overall wear volume can be measured in situ.

The main issues with the approach presented by Harden et al. are the time-based approach for measuring the ball dimensions and the measuring frequency. The authors used a timer to trigger the LPS measurements. Since the rotational frequency of the ball can fluctuate based on the grid frequency due to the use of an AC motor, the LPS does not reliably measure the same point on the ball. If the ball has a certain amount of runout, the volume calculation is fluctuating as well. Additionally, the low frequency of measurement amplifies the issue. With a measurement frequency of 0.1 Hz and a rotational frequency of the ball of 1 Hz, this means that the ball rotates ten times in between measurements. If the runout of the ball points toward the LPS in the first measurement, the calculated volume of the ball is higher than the true volume of the ball. If the ball speed is inconsistent in the delay between measurements, the LPS measures a different spot on the ball in the next measurement. If the runout in this measurement is now no longer pointing in the direction of the LPS but for example away from it, the calculated volume is lower, causing the fluctuations in the measurements seen in Table 1.

2 Methods

In this work, a Ball-on-Prism Tribometer is used for wear measurements. When testing the tribological behavior of materials on a ball-prism tribometer, typically only the wear volume of both wearing counterparts together (linear system

Table 1 Approximate noise levels of the results of Harden et al. [8]

Measurement	Noise level ball	Noise level prism
No wear	$\pm 3\text{mm}^3$	–
Only prism wear	$\pm 3.5\text{mm}^3$	$\pm 0.15\text{mm}^3$
Only ball wear	$\pm 5\text{mm}^3$	$\pm 0.2\text{mm}^3$
Both partners wear	$\pm 5\text{mm}^3$	$\pm 0.25\text{mm}^3$

wear) can be calculated. This system wear is calculated based on the indentation depth of the ball into the prism and the known geometry of both the ball and the prism.

With polymer-metal combinations, where only one partner is wearing significantly, the system wear volume is equal to the polymer wear volume. On polymer-polymer combinations, different ratios of wear volume between the ball and the prism are possible. There are two extremes to consider: Only ball wear or only prism wear. In between these two cases, the true ball- and prism wear can take any ratio. In Fig. 1, the system wear volume of a 3d printed, amorphous Poly-ether-ether-ketone (PEEK) ball wearing against a 3d printed, crystalline PEEK prism is depicted over the time. The orange curve would represent the system wear volume with the assumption of pure prism wear, the blue curve represents the system wear volume with the assumption of only ball wear. The gray area in between the two curves is the area, represents all other wear scenarios with both counterparts wearing simultaneously. In this type of measurement, a positive wear volume for the ball represents a decrease in ball-radius and for the prism wear, a positive wear volume is an increase in radius of the indentation of the ball in the prisms surface.

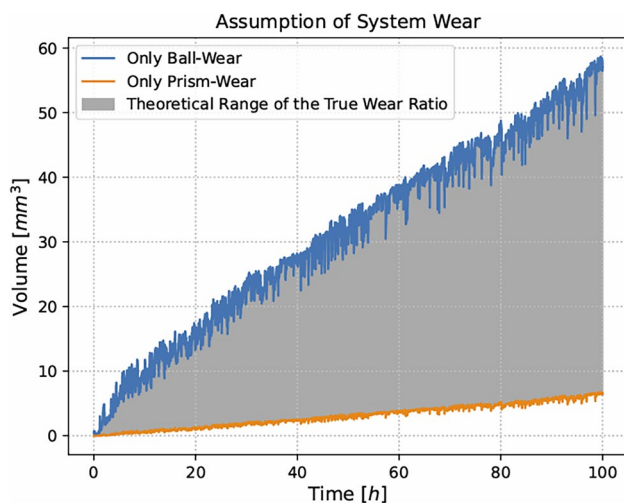
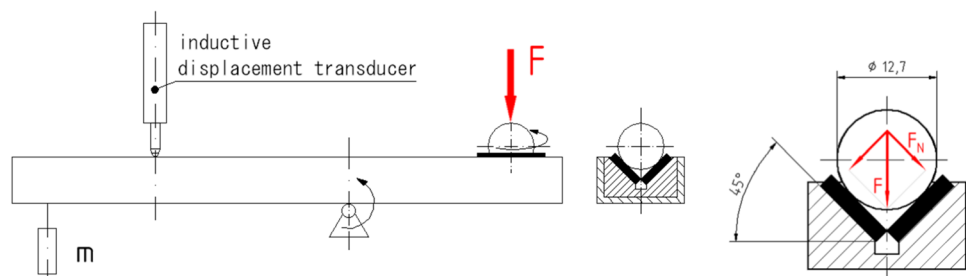


Fig. 1 System wear diagram of an amorphous PEEK ball versus a crystalline PEEK prism calculated from the indentation depth information

Fig. 2 Abstracted system diagram of the ball-prism-tribometer [14]

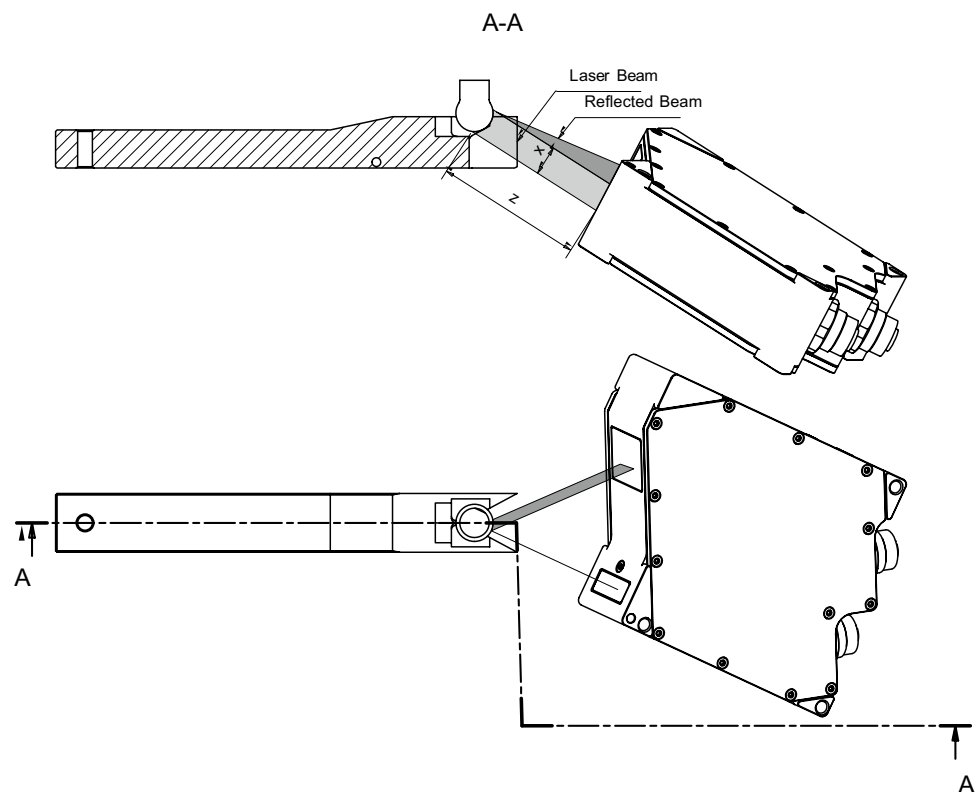


For the development of an improved in situ wear measurement system the same test- and measurement equipment was used as proposed by Harden et al. [8]. The tribological test stand used for this work is the VSP6 ball-prism tribometer by Dr. Tillwisch GmbH. This tribometer consists of levers, where the prism samples are mounted. The ball sample is clamped in a chuck, which is rotated by an electric motor. The prisms are set at a 45° angle relative to the axis of rotation of the ball. At the end of the lever opposing the ball and prism there is a weight of 500g located to apply the normal force between the ball and the prism. To translate the downward force of the weight into an upwards force of the prism on the ball, two ball bearings are used as a pivot point. The friction is then created by rotating the ball with a frequency of 1Hz, which is pressed into the prism by the normal force. To measure the indentation of the ball into the prism and vice versa, a displacement transducer is mounted, at the same distance away from the pivot point then the axis of rotation of the ball. This way there is no calculation required to obtain the correct indentation depth. The working principle of this setup is depicted in Fig. 2, alongside with the weights, the installed displacement transducer, the ball and the acting forces with the important dimensions.

The levers of the tribological test stand were modified to allow the laser beam to reach the ball during the measurement. This can be archived without changing the interaction between the ball and the prism due to the contact being present on two sides only. The cutout for the laser beam is located on the front side of the lever, which is on the right of the left most sketch in Fig. 2. The interaction of the beam and the ball can also be seen in Fig. 3 in greater detail

For obtaining the second information necessary for differentiating between the ball and the prism wear volume, a scanCONTROL 2900 10/BL LPS from Micro-Epsilon Messtechnik GmbH & Co. KG is used. The LPS consists of a line laser and an image sensor. The beam is reflected by the object to be measured and then detected by the image sensor. The sensor is located at an angle to the direction of the laser beam. This way, a change in distance of the reflection from the laser source translates to a change of the location of the reflection on the sensor. If the object, the laser beam is reflected off of, moves further away from the source, the signal on the sensor is shifted to the left (seen when looking

Fig. 3 Orientation, measuring range and dimensions of the LPS. Based on [8]



on the sensor in the direction of the reflected beam). A distance map is created on the sensor, where the distance is one dimension (z) of the sensor and the location of the object in the direction of the laser line is the other dimension (x) of the sensor. The available measurement range in the x dimension is 10.4mm the origin of the x coordinate is in the center of the measurement range. The available measurement range in the z direction spans from 52.5mm of distance away from the window where the laser is exiting to 60.5mm away from the window resulting in a measuring depth of 8mm in total. The reader may refer to Fig. 3 and Fig. 5 for a visual representation of the measuring range.

As Harden et al. proposed in their work [8], the LPS is positioned in a way that the beam hits the ball at a 30° upward angle. This is done to improve the coverage of the wear zone, which is located at the lower portion of the ball due to the prism angle of 40° relative to the axis of rotation of the ball. Additionally, the LPS is rotated by 25° clockwise around the axis of rotation to allow the laser beam to clear the prism, reach the ball and for the reflection to reach the image sensor of the LPS. This is depicted in the lower sketch of Fig. 3.

In order to increase the efficiency of the measurements, five slots of the tribological test stand are measured sequentially. To archive this, the LPS is moved by a M417.2PD Precision Linear Stage (LS) manufactured by Physik Instrumente (PI) GmbH & Co. KG. This device has a linear resolution and a unidirectional repeatability of $0.5\mu\text{m}$. This

enables the user to perform measurements on up to five different materials combinations or lubrication scenarios at the same time. Also, one can perform five tests of the same material combination simultaneously to get more statistical significant results in the same time as opposed to only measuring one slot at the time.

In order to reduce the noise of the volume measurements, the two main issues presented in the introduction of this work are addressed. To eliminate the error caused by inaccuracies in the position the LPS scans the ball, a 2RMHF3600 rotary encoder is mounted to one of the ball fixture's drive shaft. This way, the position of the ball can be obtained and can be used as the trigger. To increase the accuracy of the measurements and to eliminate the effects that the ball runout has on the measurement, the ball is scanned with a higher frequency. The LPS allows the user to reduce the size of the used sensor area, speeding up the image capturing and thus increasing the measurement frequency. This causes the available measurement range to decrease in x direction. For this particular application, the whole x -range is needed to obtain geometrical information about the full surface of the ball. This limits the maximum frequency up to 140Hz . The measurement is triggered by the z -disk of the encoder, which pulses once per rotation. The ball is then scanned with about 100Hz until the z -pulse is triggered again. This way, exactly one rotation is measured and the scan yields up to 140 profiles which are saved as CSV files containing the x , z

data of each profile. In order to save computing resources, and disk space, the frequency can be set as a user input. A high number of profiles per rotation effectively eliminates the effects of the runout or "wobble" of the ball during rotation because sections where the ball is coming toward the LPS are canceled with the section on the opposite side of the ball where it moves away from the LPS. Also balls, which have an error in roundness can be measured more accurately. A visual representation of this can be seen in Fig. 4.

Instead of using LabView by National Instruments, the data capturing and processing, as well as the controlling of the LPS, linear axis and encoder is done by a Raspberry Pi 5. The software is written in Python 3. The main reason behind this is that there is a Python software development kit available for all the components. This way, the control of the whole system can be done by the Raspberry Pi 5 and features can be added quickly. The only limitation of this approach is that the data coming from the linear displacement transducer can only be exported as an ASCII file on a Windows machine. Since the final calculation is meant to be done by a sophisticated workstation, the ASCII file has to be exported together with the data from the LPS.

On the right sketch of Fig. 4 the effect of runout combined with a roundness error on the approach presented by Harden et al. is shown. In this case the LPS measurement (blue line) is taken right when the ball reaches its furthest point from the LPS. The calculation method calculates the volume smaller than the actual volume, when the measured surface is further away from the LPS. This might be the case when the ball center is behind the axis of rotation (away from the LPS) or when the slimmer part of an oval ball is measured. Conversely, the calculation method yields a volume, which is higher than the actual ball volume when

the ball center is closer to the LPS than the axis of rotation or the thicker part of the oval is pointing toward the LPS.

On the left Fig. 4 the developed approach can be seen. For simplicity's sake, the figure is simplified to only show six ball segments. This would correspond to a LPS frequency of 6Hz and a rotational velocity of 1Hz. During real, full speed measurements with a rotational velocity of 1Hz this would result in 100 ball segments, the volume of which is calculated individually and added up to the overall volume of the ball. With this approach, runout and roundness error are canceled out because more geometrical information is obtained during the measurement. This discretized approach increases in accuracy with a rising number of segments.

Instead of manually calibrating the axis of rotation for every slot before every measurement, the axis of rotation is calculated from the generated profiles of the first rotation from the measurement, where the practically unworn ball shape is measured. For each profile of the first revolution yielding a scan with a sufficient number of valid profiles, a circle fit is performed using the NumPy function "curve_fit" with:

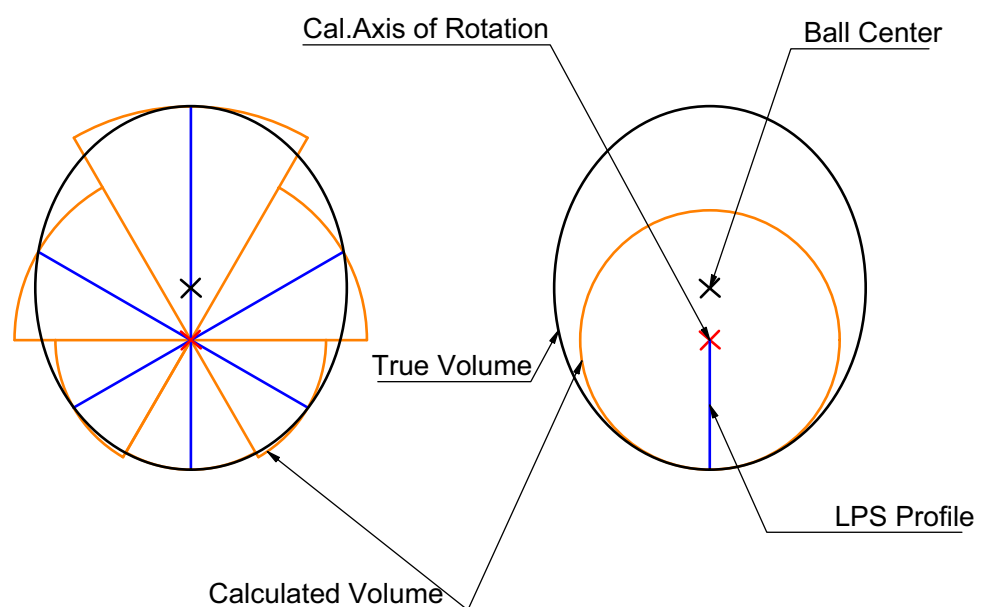
$$0 = (x_c - a)^2 + (z_c - b)^2 - r^2 \quad (1)$$

where:

- x_c : x – coordinate of point from LPS
- z_c : z – coordinate of point from LPS
- a : x – coordinate of the center of the circle
- b : z – coordinate of the center of the circle
- r : radius of the circle

which yields the center point of each profile and the respective radius. The standard deviations for all variables are also

Fig. 4 Simplified 2-D representation of the effect of runout and roundness error on calculation (left developed approach and right the approach presented by Harden et al.)



calculated to verify the accuracy of the calculations. Since the LPS is pointed directly at the axis of rotation, the center points correlate with the center point of the ball. The resulting center points are then averaged to get the center point of the ball in both x and z direction.

2.1 Calculation of Wear Volumes

The equations for the calculation of the wear volume from the approach that Harden et al. [8] proposed are adapted and expanded to account for the full-rotation-scan the developed method uses.

The data needed for the calculation of the wear volumes of both the ball and the prisms is the contour of the ball, obtained by the LPS and the indentation depth, measured by the linear displacement transducers. The ball is discretized into stacked, truncated cones with a certain height $h_i(t)$ and radius $r_i(t)$. Figure 5 serves as a visual reference for a better understanding of the dimensions and the calculation. $H_i(t)$ is the x coordinate of the LPS with H_0 being the x coordinate of the intersection between the ball and the axis of rotation. $l_i(t)$ is the z coordinate of the LPS at $H_i(t)$ and resembles the distance between the LPS and the surface of the ball. L is the z coordinate at H_0 .

The height of each individual stacked cone making up the ball is calculated by transforming the distance between two x coordinates ($H_i(t) - H_{i+1}(t)$) into a horizontal distance or height $h_i(t)$:

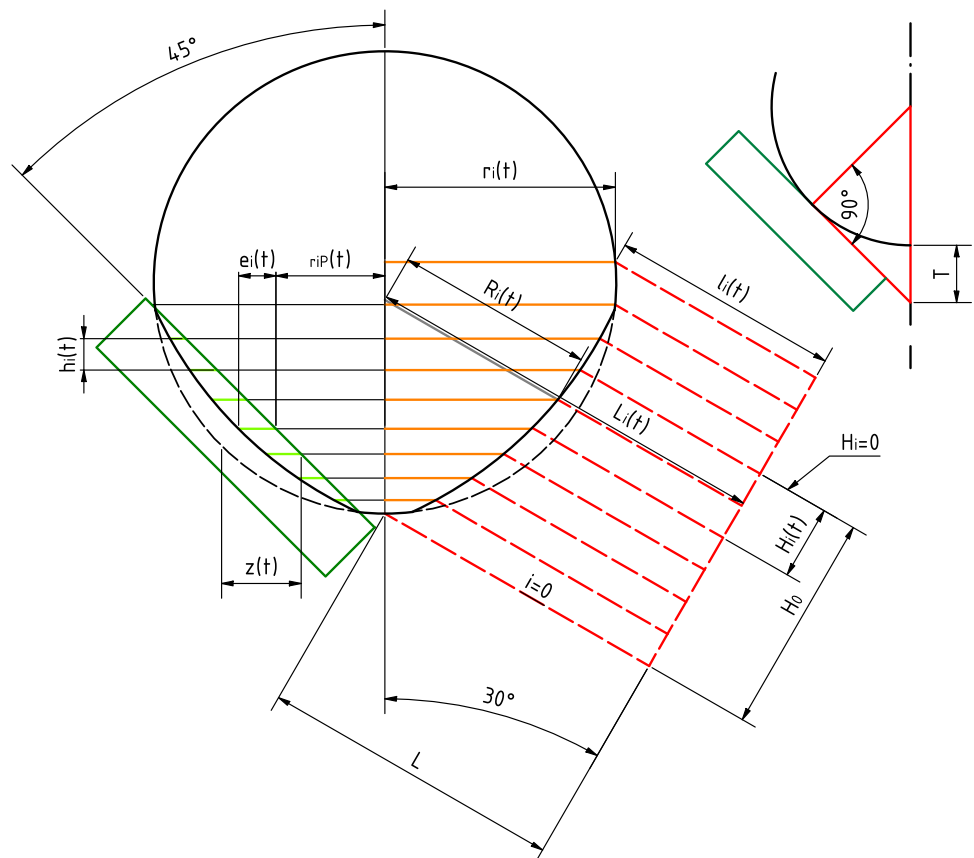
$$h_i(t) = \cos(\alpha) \cdot (H_i(t) - H_{i+1}(t)) + \sin(\alpha) \cdot (l_i(t) - l_{i+1}(t)) \tag{2}$$

where,

$$\alpha = 30^\circ$$

From the known angle of the LPS and the calculated center point of the ball coming from the circle fits for all profiles of the first revolution, the axis of rotation is defined as a line, which is tilted by 30° relative to the local coordinate system of the LPS. This results in a vertical axis through the center point and the tip of the ball. With this known axis of rotation the tip of the ball is defined as the intersection point of the axis of rotation and the fitted circle. The data from the LPS is truncated at the x coordinate of the ball tip to avoid measuring past the tip of the ball. The first point in the LPS data near the tip is then L . With the known tilt angle α , every horizontal radius $r_i(t)$ of each cone making up the discretized ball can be calculated with the following basic geometric relationships seen in Fig. 5:

Fig. 5 Relevant dimensions for the calculation of wear volumes, based on [8]



$$L_i(t) = L + \tan(\alpha) \cdot [H_0 - H_i(t)]$$

$$R_i(t) = L_i(t) - l_i(t)$$

$$r_i(t) = R_i(t) \cdot \cos(\alpha)$$

to result in:

$$r_i(t) = L \cdot \cos(\alpha) + \sin(\alpha) \cdot [H_0 - H_i(t)] - l_i(t) \cdot \cos(\alpha). \quad (3)$$

When summing up the truncated cones that make up the discretized ball, one receives the current ball volume for the measured section. For this the height and the radii of the cones from Eqs. (2) and (3) are needed.

$$V_k(t) = \frac{\pi}{3} \sum_i h_i(t) \cdot [r_i(t)^2 + r_i(t) \cdot r_{i+1}(t) + r_{i+1}(t)^2] \quad (4)$$

The wear volume is defined as the difference between the volume at the start of the experiment ($t = 0$) and the current volume. With this definition, the wear volume of the ball over time is given by:

$$\Delta V_k(t) = V_k(0) - V_k(t) \quad (5)$$

For the calculation of the wear volume of the prisms, the indentation depth data from the displacement transducer $z(t)$ is needed. Due to the 45° angle of the prisms relative to the axis of rotation, a change in height corresponds to the same change in distance to the unworn prism surface. This means that the horizontal distance from the axis of rotation $r_{iP}(t)$ to the unworn prism surface can be calculated with a known $h_i(t)$ from Eq. 2 by adding the change in height to the height of the tip of the ball r_{0P} .

$$r_{iP}(t) = r_{0P}(t) + \sum_{i=0}^n h_i(t) \quad (6)$$

with,

$$r_{0P}(t) = T - z(t)$$

With the information about the indentation depth and the ball shape, the real wear volume of the prisms can be determined. The traditional measurement method without the LPS implies that the indentation in the surface of the prism is also ball-shaped. This is true only if there is no ball wear. When the ball starts wearing, the results deviate from their true value because the indentation of the ball into the prism turns from a ball segment into a cylinder segment since the ball turns into a cone. Because the prism is stationary and the shape of its wear indentation is not a function of the rotational position of the ball but only of the experiment time, only one profile is used to determine

the shape of the indentation. For the calculation of the wear volume of the prisms, the difference of the distance between the axis of rotation and the surface of the unworn prism $r_{iP}(t)$ and the current ball radius $r_i(t)$ is defined as $e_i(t)$ (light green area). The calculation of the wear volume is done in a similar manner, as the calculation of the wear volume of the ball. Instead of summing up full cylinders with the height $h_i(t)$ and a radius $r_i(t)$, the wear volume is calculated by summing up cylinder segments with the depth $e_i(t)$, the radius $r_i(t)$ and the height $h_i(t)$.

$$\Delta V_p(t) = 2 \sum_i h_i(t) \left[\{r_i(t)\}^2 \cdot \arccos \left(1 - \frac{e_i(t)}{r_i(t)} \right) - r_i(t) \cdot \sqrt{2 \cdot r_i(t) \cdot e_i(t) - \{e_i(t)\}^2} \right] \quad (7)$$

with,

$$e_i(t) = r_i(t) - r_{iP}(t)$$

leads to,

$$\Delta V_p(t) = 2 \sum_i h_i(t) \left[\{r_i(t)\}^2 \cdot \arccos \left(\frac{r_{iP}(t)}{r_i(t)} \right) - r_i(t) \cdot \sqrt{r_i(t)^2 - r_{iP}(t)^2} \right]. \quad (8)$$

Equation 7 is the sum of all volumes of the cylinder segments multiplied by two, since there are two prisms with equal wear. Equation 8 is the simplified and substituted version of Eq. 7. For all the following measurements, the ball wear volume is positive, as the radius of the ball decreases with wear. The prism wear volume however is now defined as negative, as the prism wears. This is because the radius of the indentation essentially increases. The reference of positive wear volume is defined as ball wear, so if the ball would increase in radius, the wear volume would be negative. This is why the prism wear volume is now defined as negative as wear occurs. Please note however that in case of material transfer, which is not considered wear according to the third body model, the laser would pick up the prism material on the ball and would recognize it as a negative wear volume since the balls radius would increase.

In terms of material balance, the removed material from the ball and the prism could be retained in the system, for example in the form of a transfer film or particles in the contact region. This would show up as a falsely increasing ball volume. The material could also circulate between the two bodies which would create an increase in noise. Finally, the removed material could be ejected from the system, which results in a change in ball- or prism-volume. The presented approach is mainly intended to detect the amount of ejected material form the ball and the prism.

In cases of a large amount of retention or circulation can result in false measurements.

2.2 Error Filtering

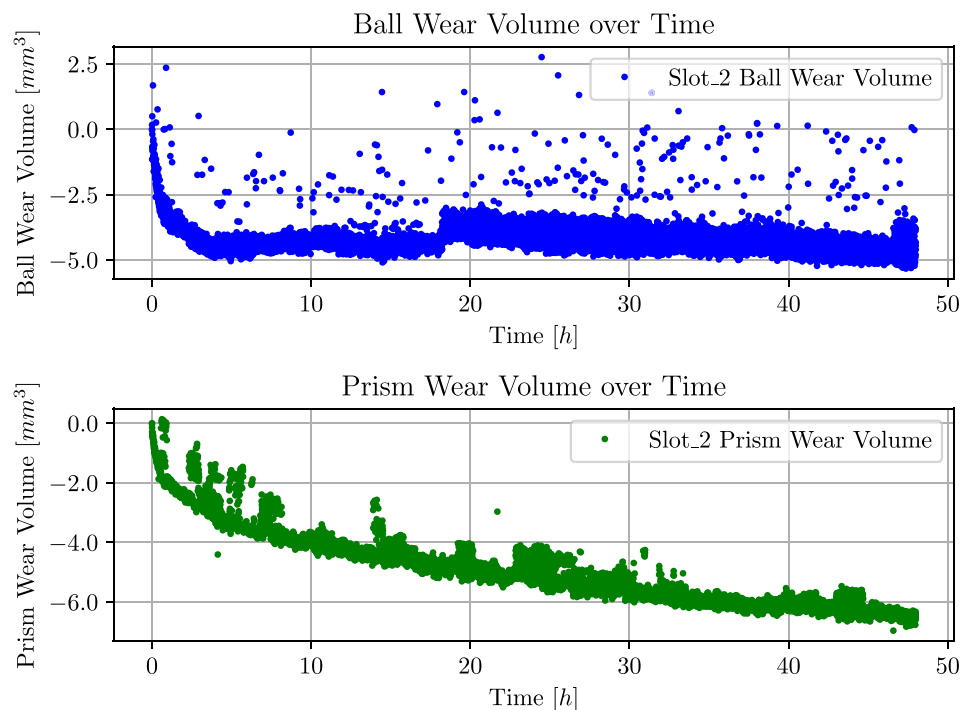
The fact that the ball volume is obtained by scanning its surface creates the weakness of false measurements when debris accumulates on the ball. In the third body approach, presented by Godet et al. [5], this debris is considered to resemble a third body, that once left the first bodies and now is free to move around in the wear system. These bodies can influence the wear behavior by forming a lubrication film or transferring the normal forces between the wearing bodies [5]. These particles are measured by the laser and are then considered to be part of the ball volume. This can lead to temporary errors in the calculation of the ball wear volume. This aspect cannot be improved by the error filtering in our approach. If the particle is reflecting the light in a way that not enough - or too much - light is hitting the sensor, the LPS either does not produce a data point at all or it measures a radius smaller than in reality producing a spike in the profile data. This in turn would cause the wear volume to produce a sharp spike in the positive direction of the wear volume. In Fig. 6 the unfiltered data are depicted. This is the unfiltered data of an Aluminum ball, which shows no wear, against a prism made from 3D printed iglidur® i150 filament. To increase the diffuse reflectiveness of the ball, its surface was roughed by using 1000 grid sandpaper. The outliers that can be seen in Fig. 6 are due to a thin transfer film of the prism material temporarily filling the roughness

on the balls surface and hindering the beam from entering the sensor correctly. This causes a spike in positive wear direction, as explained earlier in this work. The steep decline in the ball wear volume is the expansion of the test stand as well as the laser assembly itself during warm-up. This can be mitigated by letting the laser pre-run, getting it to operating temperature before placing the prism onto the Ball-Prism Tribometer and starting the measurement.

In order to filter out the outliers, two operations are performed on the data. First, before the computation of the wear volumes, each profile is checked for sudden jumps of the data points where $|l_i(t) - l_{i+1}(t)| > k$ with k being the threshold at which a jump in the profile data is detected as an invalid point and deleted from the data. This threshold is set to 0.2mm in this work. This value was chosen because it is sufficiently large to preserve all information about the surface but cut out all spikes where data are invalid since these spikes jump about $\pm 0.5 - \pm 2\text{mm}$. This cleaning of the data before performing computations on it is also important for the calculation of the rotational axis on the first, unworn revolution since any invalid data points can have an impact on the rest of the volume calculation due to an error in the calculation of the center point of the ball. This first cleaning step reduces the number of extreme outliers, appearing multiple cubic millimeters away from the mean of the data. These can be seen in Fig. 6 on the ball wear volume chart.

The second cleaning is done after the calculation of the wear volumes and aims to smooth out spikes in the volume data caused by debris on the ball, which is not producing a single spike in the laser profiles but instead a temporary

Fig. 6 Unfiltered data of aluminum ball wear and iglidur® i150 prism wear



bulge on the surface. These kinds of inaccuracies are not filtered in the first cleaning of the unfiltered data and are carried through into the calculation of the wear volumes. Another source of inaccuracies is the noise and defects in the data provided by the displacement transducer of the ball-prism tribometer. These defects manifest themselves not just as single point outliers but as accumulations of points widening the noise level in the prism data and producing smaller spikes containing multiple points. The fact that this is coming from the displacement transducer is underlined due to this behavior also being observable in the traditional measurement approach shown in Fig. 1. The second smoothing method works similar to the first one but instead of deleting the points, they are shifted toward the mean of the two neighboring points before and after the detected outlier. The detection works by $|V_i(t) - V_{i+1}(t)| > m$ with m being the threshold at which the outlier is shifted to the mean of its nearest two neighbors. m can have a start- and an end-value and by providing a number of iterations, the filtering process is repeated iteratively with m getting smaller each iteration. This way, in the beginning of the filtering, extreme outliers are filtered and lose their impact on later iterations. As m gets smaller, the less significant outliers are shifted toward the mean of the wear volume over time and finally, the noise level is compressed around the mean of the noise level. For this work, m is reduced from 1 to 0.01mm^3 within 250 iterations. Figure 7 shows the algorithm being applied to the unfiltered results shown in Fig. 6. In these final result plots, also a simple moving average (SMA) is shown, which was calculated in post-processing of the raw data. This resembles

the final, smoothed measurement curve that can be analyzed and compared to other measurements to gain a better understanding of the measurement. The window length of the SMA can be set by the user and is preset to a length of 200 as shown in the following figures. The SMA is calculated using the filtered data. An example for using the obtained measurements would be to calculate the surface pressure between ball and prism where the wear significantly tapers off. One could also calculate specific wear rates based on the obtained data.

3 Results

In order to compare the approach proposed by Harden et al. to the process introduced in this work, wear tests are conducted using a ball with no counterpart to create zero wear, an aluminum ball against a polymer prism to create only prism wear and a polymer ball on a steel prism to only create ball wear. The noise levels are obtained by approximating the amplitude of the noise where no visible defect (eg. debris) is present in the data. The chosen filtering method for the presented results is chosen based on what approach yielded the best overall result. This depends on the type of wear and the amount of mean shift. Figures 8, 9, 10 and 11 show the final results of the measurements. The approach presented in this work is capable of differentiating between ball and prism wear, even when both partners wear simultaneously. Table 2 compares the noise levels of the results presented in this work and the results presented in the previous

Fig. 7 Final Results of Aluminum Ball wear and iglidur® i150 prism wear

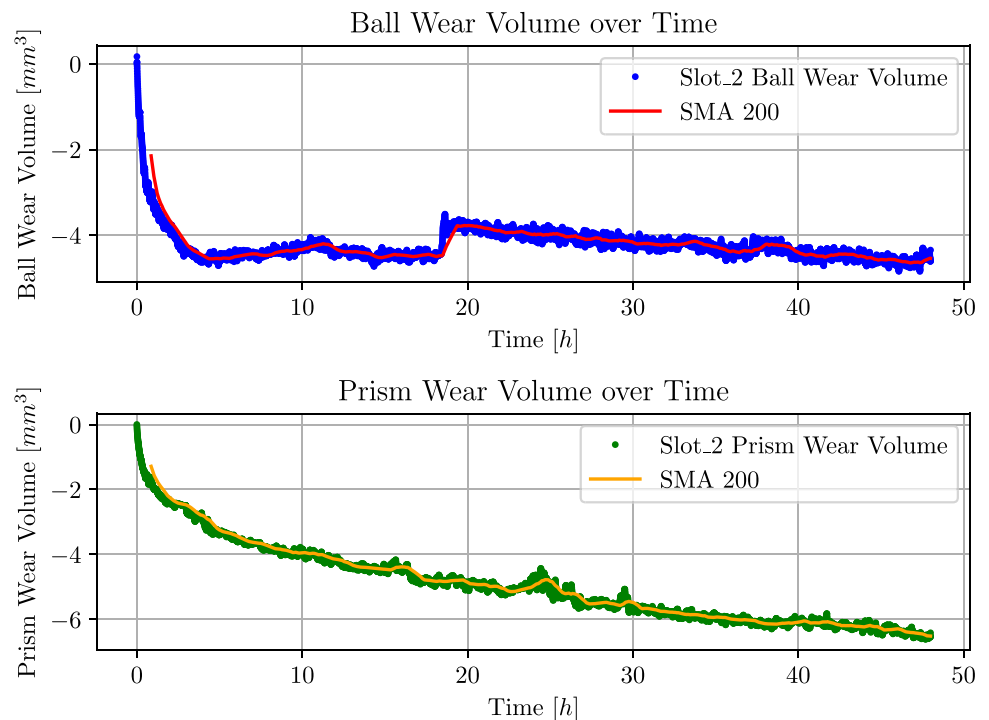


Table 2 Approximate noise levels of the presented approach with filtering and level of improvement compared to the approach of Harden et al. [8]

Measurement	Noise Level Ball	Noise Level Prism	Imp. % Ball	Imp. % Prism
No wear	$\pm 0.1mm^3$	–	97%	–
Only prism wear	$\pm 0.2mm^3$	$\pm 0.15mm^3$	94%	0%
Only ball wear	$\pm 1mm^3$	$\pm 0.5mm^3$	80%	– 50%
Both partners wear	$\pm 0.1mm^3$	$\pm 0.15mm^3$	98%	40%

Fig. 8 Final, filtered results of only a 3D printed ball rotating without a prism installed

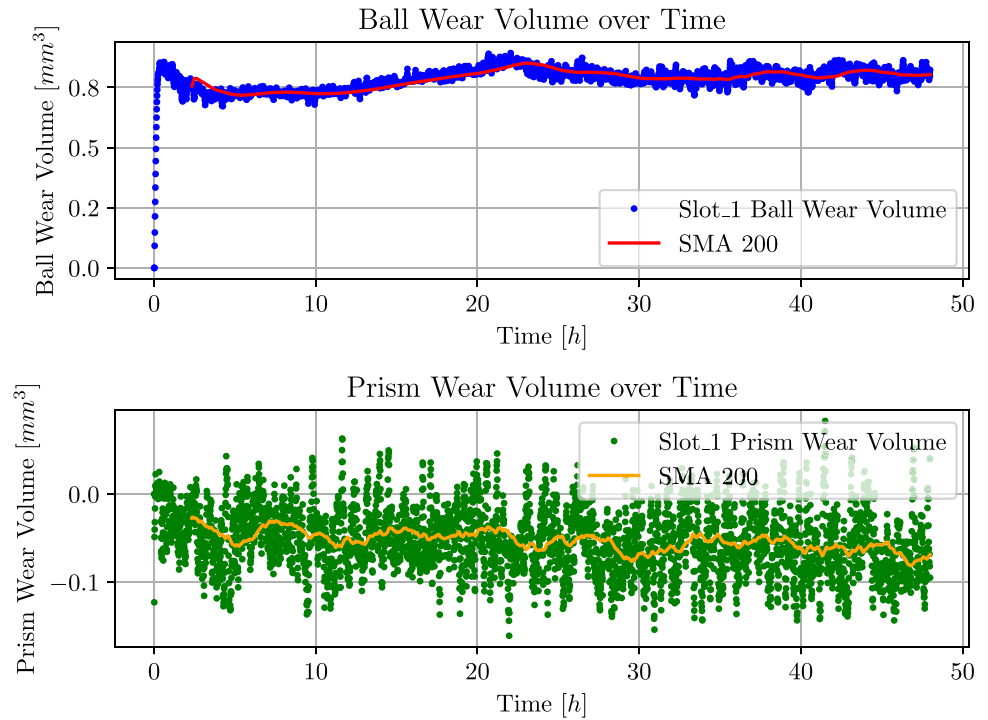


Fig. 9 Final, filtered results of a 3D printed iglidur® i150 ball wearing on a steel prism

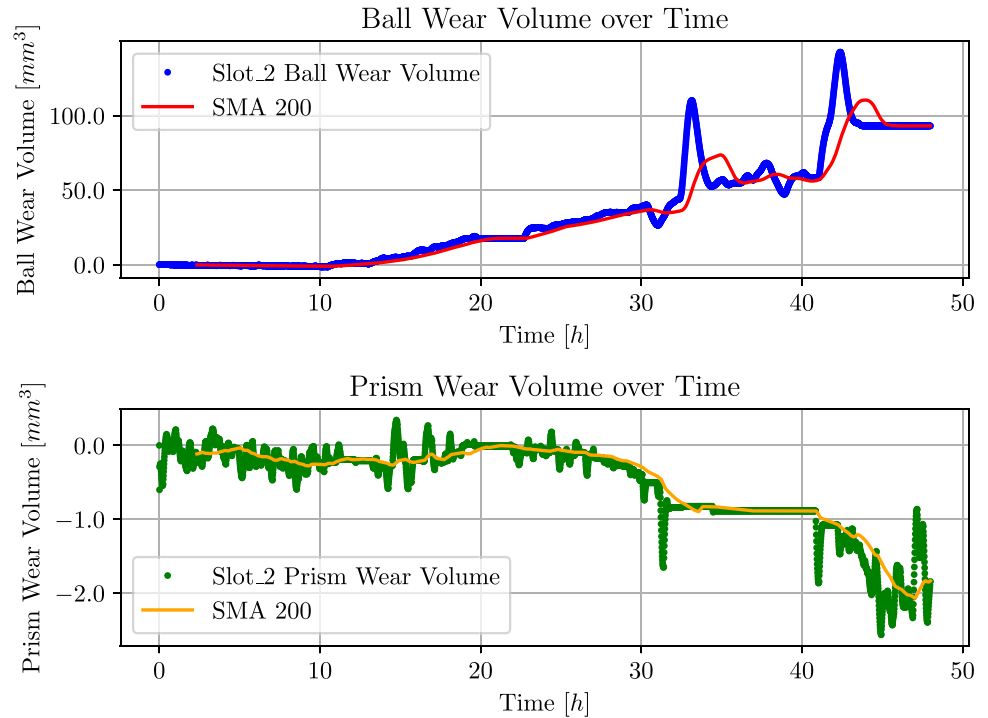


Fig. 10 Final, filtered results of a 3D printed iglidur® i150 ball wearing on a PLA prism

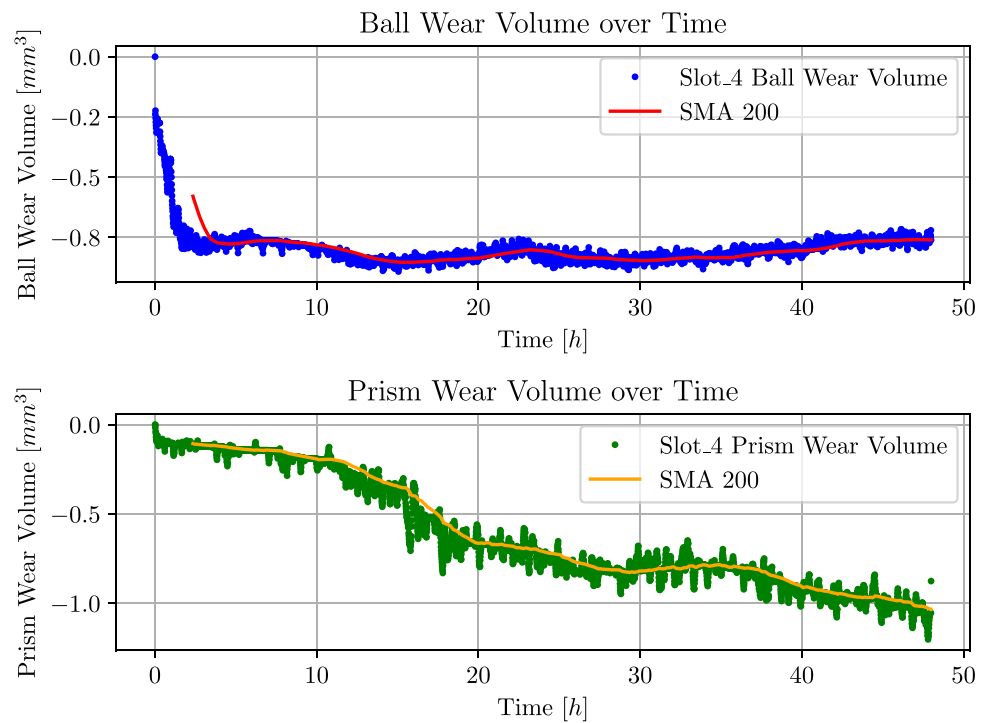
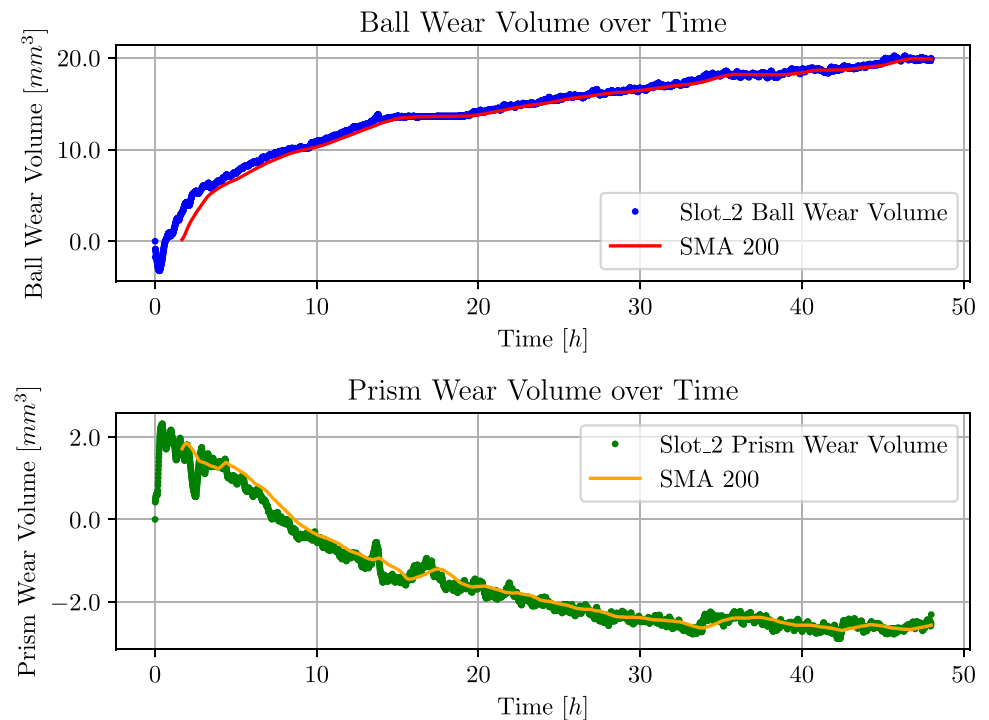


Fig. 11 Final, filtered results of a 3D printed PLA ball wearing on an amorphous PEEK prism

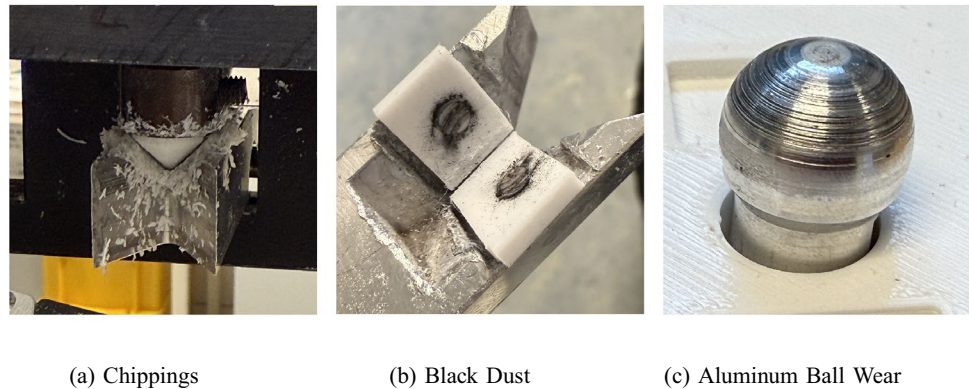


work of Harden et al. [8]. The results in Table 2 are read from the graphs before significant failure of the samples. The noise level can significantly increase once a sample-failure occurs. The material combinations used in this work were not specifically chosen to produce a small amount of debris to enhance the quality of the measurements but are chosen to better show the real-world results.

Figure 7, used as an example for the filtering algorithm, shows the result of an aluminum ball wearing against an iglidur® i150 prism.

In fast wearing combinations, such as shown in Fig. 9, a significant buildup of dust and debris occurs on the prism mount, see Fig. 12a for reference. Some combinations even show chips of ball material instead of simple dust. If the

Fig. 12 Wear Phenomena



wear in 3d printed samples reaches a magnitude where the infill of the print is exposed, wear and debris-buildup increases drastically.

4 Discussion and Outlook

The improved approach for measuring the wear in polymer-polymer combinations presented in this work reduces the noise and subsequently increases the accuracy significantly. With a given accuracy of the LPS of $0.5\mu\text{m}$, the volume accuracy for a half sphere, which is roughly the area, the LPS covers, is about 0.13mm^3 for a ball with a diameter of 12.7mm . The error in the volume would increase with a larger radius since the radius is cubed in the equation for the volume of a sphere. This corresponds with the noise levels in Table 2, however this does not mean, that the rest of the system is effectively noise free, since the final data are smoothed. The noise in the prism data roughly stayed the same since there were just performance improvements for the measurement and the calculation made. The main-improvements come from the changes in the ball-measurements. The presented results show that the measurement technique is able to differentiate between ball- and prism wear. The warmup period of the LPS still presents an issue despite letting the LPS idle several hours before starting the measurement. To combat this behavior, a warm-up script could be used where the LPS is measuring temporary data at maximum capacity for a few hours. Once the LPS reaches equilibrium temperature, the measurement could be started.

Figure 7, which shows the results of an aluminum ball wearing against the iglidur® i150 prism, showed a small amount of ball wear after warm-up. This is counter-intuitive since the aluminum ball should not show any signs of wear against the polymer prism. However, upon further inspection of the specimen after the measurement, the aluminum ball showed signs of wear in the form of black dust

and wear-grooves on the surface of the ball. The (white) prism showed a buildup of the black dust as well. Pictures of this can be seen in Fig. 12b and c.

In Fig. 9, which is showing the results of the 3d printed iglidur® i150 ball against a steel prism, one can observe a kink in the ball wear volume around the 10 h mark. This is the point where the ball starts wearing significantly. At this point, the ball started shedding off small chips of material. This can be seen in Fig. 12a. These chips of polymer started to accumulate on the ball, the prism and on the LPS, which caused an increase of the noise. However, despite the increase in noise, the 200 period SMA stayed around zero wear volume up until 28 h into the measurement. At this point, the measurement became unreliable due to the ball degrading rapidly, throwing off the calculation. This is not considered an issue with the approach, since in real application the material combination would have been declared unfeasible when the failure of the ball occurred around hour 10-20. In order to reduce the effects of debris-buildup on the prism holder, a compressed air line could be installed close to the ball, blowing short bursts of air to remove the dust. If these bursts of air are sufficiently short, there would not be a significant cooling effect, which could alter the wear conditions or the results. These particles have already left the wear zone, and are thus not considered as a third body anymore. Technically, the particles could enter the wear system again, but since the buildup is happening between the ball and the laser, only blocking the laser path, they are still no longer considered third bodies. This air could however also blow away dust and particles that are still on the interface of the ball or the prism, which could alter the wear behavior.

Figure 10 shows the results of a material combination that shows only minimal wear during the span of the experiment. One can see that the quality of the measurement improves as lower amounts of debris is accumulating. After the experiment, almost no indent was visible on the prism surface and

the ball only showed a smoother and shinier surface where it made contact with the prism.

Figure 11 shows a PLA ball wearing on an amorphous PEEK prism with a ball wear amount of around 20mm^3 in 48 h and a prism wear of around 4mm^3 in 48 h. This would resemble a practical material combination in testing.

The presented approach deviates from the third body approach since the third bodies that are present on the ball, are considered part of the ball volume. This can potentially lead to errors in the ball volume calculation since the volume of the third bodies simply gets added to the volume of the ball. Experiments conducted with a high amount of third body particles show an increase in noise due to the temporary nature of these particles and transfer films in with the materials used for the experiments. The process would greatly benefit from an added detection algorithm for detecting the third body transfer layers and particles on the ball. For this an algorithm would be necessary that can detect said surface behaviors using only topographic data from the LPS.

One limitation of the optical approach is, the limited performance on transparent and semi-transparent ball-materials, since they do not provide a clear image on the sensor due to light absorption and reflections inside the ball. A possible addition to the measurement setup could be an IR camera to capture data of the temperature on the surface of the ball right when it comes off of the prism surface. This would not be indicative of the real contact temperature but can serve to better understand certain wear behavior in polymer-polymer tribo-systems. This addition could potentially yield more information about the sudden shifts and changes in the wear volume, such as seen in Fig. 9.

Author Contributions PC.S wrote the main manuscript, prepared the figures, developed the method and did data interpretation. B.S., R.K. and R.A. did data interpretation. All authors reviewed the manuscript and accepted the manuscript for submission.

Funding Open Access funding enabled and organized by Projekt DEAL. The authors have not disclosed any funding.

Data Availability No datasets were generated or analysed during the current study.

Declarations

Conflict of interest The authors declare no conflict of interest.

Open Access This article is licensed under a Creative Commons Attribution 4.0 International License, which permits use, sharing, adaptation, distribution and reproduction in any medium or format, as long as you give appropriate credit to the original author(s) and the source,

provide a link to the Creative Commons licence, and indicate if changes were made. The images or other third party material in this article are included in the article's Creative Commons licence, unless indicated otherwise in a credit line to the material. If material is not included in the article's Creative Commons licence and your intended use is not permitted by statutory regulation or exceeds the permitted use, you will need to obtain permission directly from the copyright holder. To view a copy of this licence, visit <http://creativecommons.org/licenses/by/4.0/>.

References

1. Sinha, S.K., Briscoe, B.J.: *Polymer Tribology*. Imperial College Press, London and Singapore (2009)
2. RYMUZA, Z.: Tribology of polymers. *Arch. Civil Mech. Eng.* **7**(4), 177–184 (2007). [https://doi.org/10.1016/S1644-9665\(12\)60235-](https://doi.org/10.1016/S1644-9665(12)60235-)
3. Santner, E., Czichos, H.: Tribology of polymers. *Tribol. Int.* **22**(2), 103–109 (1989). [https://doi.org/10.1016/0301-679X\(89\)90170-](https://doi.org/10.1016/0301-679X(89)90170-)
4. igus-GmbH: igus Website. <https://www.igus.eu/3d-print-material/3d-print-filament> Accessed 11 Jul 2024.
5. Godet, M.: Third-bodies in tribology. *Wear* **136**(1), 29–45 (1990). [https://doi.org/10.1016/0043-1648\(90\)90070-Q](https://doi.org/10.1016/0043-1648(90)90070-Q)
6. Gee, M.G., Owen-Jones, S.: *Wear Testing Methods and their Relevance to Industrial Wear Problems* (1997)
7. Albawab, T.M.M., Umar Nirmal, Halim, I., Salem, M.A., Elsayed, M., Singh, J. (2018) A review on tribological wear test rigs for various applications. *Int. J. Integr. Eng.* <https://doi.org/10.30880/ijie.2018.10.08.030>
8. Harden, F., Schädel, B., Siegel, M., Kral, R., Adelung, R., Jacobs, O.: Proof of concept: in-situ wear differentiation of simultaneously wearing counterparts. *Tribol. Lett.* **71**(3), 1–14 (2023). <https://doi.org/10.1007/s11249-023-01759->
9. Harden, F., Schädel, B., Kral, R., Siebert, L., Adelung, R., Jacobs, O (2021) Wear behavior of additive manufactured polymer-polymer sliding combinations. *Tribologie und Schmierungstechnik* **68**(2): 15–26. <https://doi.org/10.24053/TuS-2021-0010>
10. Khosla, V., Doe, N., Xiao, J., Chan, M., Char, G.: Apparatus for In-line Testing and Surface Analysis on a Mechanical Property Tester. US10024776B2. Rtec-Instruments Inc (2016)
11. Khosla, V., Doe, N., Chan, M., Xiao, J., Char, G.: Method for In-line Testing and Surface Analysis of Test Material with Participation of Raman Spectroscopy. US10258239B2. Rtec-Instruments Inc (2017)
12. Peng, W.T., Ping, Y., Xiaogang, Z., Le, Z.: Abrasion In-Situ Measuring Device Based on Digital Image Processing and Method. CN102607977B. Xi'an Yongze Huazheng Information Technology Co.,Ltd (2012)
13. Dongfeng, D., Lizhang, Z., Xue, F.: Friction Wear Testing Machine for On-line Measurement. CN101504357A. Xian Jiaotong University (2009)
14. Schädel, B., Rüdiger, G., Jacobs, O., Arzer, I., Eschner, U.: Auswirkung verschiedener Nanopulver (NanoVit) im Epoxidharz auf den Verschleiß. *GfT-Conference Publications* (2007)

Publisher's Note Springer Nature remains neutral with regard to jurisdictional claims in published maps and institutional affiliations.